CONICAL TECHNIQUES

FOR INCOMPRESSIBLE NON-VISCOUS FLOW

Thesis by

Allen I. Ormsbee

In Partial Fulfillment of the Requirements

For the Degree of

Doctor of Philosophy

California Institute of Technology

Pasadena, California

1955

ACKNOWLEDGMENTS

The writer wishes to express his gratitude to Dr. H. J. Stewart for his guidance and advice in carrying out this work, and to Dr. R. H. Edwards of the Hughes Aircraft Company for his valuable assistance in interpreting the results of this study.

Sincere thanks are also given to Mrs. M. Wood for the excellent drawings contained in this work, and to Mrs. H. Van Gieson for her skillful preparation of the manuscript.

In addition, the writer expresses his grateful appreciation to the Hughes Aircraft Company and to the Howard Hughes Fellowship Program, under whose sponsorship the writer's graduate study program was carried out.

ABSTRACT

An analytical investigation was made of incompressible potential flow fields in which the velocity components are homogeneous of order zero. Superpositions of such fields were then made and expressions were derived for the flow fields associated with constant-strength source and vortex sheets of finite extent.

The constant strength source-sheets were then applied to the construction of aerodynamic models of thin non-lifting wings of polygonal planform and airfoil section.

By use of the constant strength vortex-sheets, several approximate aerodynamic models were constructed for the determination of the pressure distribution on thin lifting wings at small angles of attack.

TABLE OF CONTENTS

LIST OF FIGURES

NOMENCLATURE

a,b,c	real constants
i,j,m,n,s	indices
P	$-\frac{2u}{q}$ pressure coefficient
q	free stream velocity
r	$\sqrt{x^2+y^2+z^2}$ = radial distance from origin in xyz space
t	wing thickness per unit chord
U,V,W	complex velocity functions
u	Rl(U); the real perturbation velocity component parallel to the x axis
v	Rl(V); the real perturbation velocity component parallel to the y axis
w	Rl(W); the real perturbation velocity component parallel to the z axis
u*	Im(U)
v*	Im(V)
w*	Im(W)
x,y,z	Cartesian coordinates in physical space
α	wing angle of attack
ϵ	(y+iz)/(x+r)
ξ	Rl(ϵ) = y/(x+r)
η	Im(ϵ) = z/(x+r)
λ	dimensionless spanwise coordinate
θ	dimensionless chordwise coordinate

I. INTRODUCTION

This work is concerned with the properties of those solutions to the subsonic three-dimensional potential flow equations which are homogeneous of order zero.

Donkin[1] has shown that the general homogeneous solution of order zero to the Laplace equation may be written in the form

$$S = F(\epsilon) + G(\bar{\epsilon}) \tag{1}$$

where $\epsilon = \dfrac{y + iz}{x + \sqrt{x^2 + y^2 + z^2}}$,

$\bar{\epsilon}$ is the complex conjugate of ϵ ,

and G and F are arbitrary functions.

Jones[2] and Lampert[3] have studied subsonic potential flow fields in which the velocity components (u, v, w) are homogeneous of order zero, and by superposing certain of these fields, were able to obtain flows satisfying certain of the boundary conditions for a finite body. Their basic solutions were improper however, due to the presence of extraneous sidewash and/or downwash discontinuities, and as a result some of their finite body solutions fail to satisfy the correct boundary conditions far upstream of the body.

Flow fields in which the velocity components are homogeneous of order zero, so-called 'conical' flows, are characterized chiefly by the appearance of sheet disturbances (e.g., source sheets or vortex sheets) which cover infinite planar sectors in space, and line disturbances (e.g., line sources or vortices) which have a linear variation of strength and

extend to infinity. Their direct physical significance is questionable since the absence of a characteristic length permits no insight into the nature of the flow at 'large' distances from such disturbances.

It can be shown however, that under certain circumstances, proper superposition of such flows, in which a characteristic length is introduced, reduces the extent of the disturbances and allows a discussion of the flow at large distances from such disturbances. In these cases, the appropriate boundary conditions can be applied.

In the present treatment, complex conical 'velocity functions' (U, V, W) are defined, the real parts of which represent the physical velocity components (u, v, w). Relations governing U, V, and W are derived, restrictions are discussed on the types of singularities these functions may have, and techniques are developed for the superposition of conical fields to obtain non-conical, physically significant flows. Several specific conical fields are discussed, and superpositions of these fields are made to provide examples of three-dimensional fields of interest to the aerodynamicist. Two of these examples are then used to construct models of lifting wings and techniques for handling these models are discussed.

extend to infinity. Their direct physical significance is questionable since the absence of a characteristic length permits no insight into the nature of the flow at 'large' distances from such disturbances.

It can be shown however, that under certain circumstances, proper superposition of such flows, in which a characteristic length is introduced, reduces the extent of the disturbances and allows a discussion of the flow at large distances from such disturbances. In these cases, the appropriate boundary conditions can be applied.

In the present treatment, complex conical 'velocity functions' (U, V, W) are defined, the real parts of which represent the physical velocity components (u, v, w). Relations governing U, V, and W are derived, restrictions are discussed on the types of singularities these functions may have, and techniques are developed for the superposition of conical fields to obtain non-conical, physically significant flows. Several specific conical fields are discussed, and superpositions of these fields are made to provide examples of three-dimensional fields of interest to the aerodynamicist. Two of these examples are then used to construct models of lifting wings and techniques for handling these models are discussed.

II. THE CONICAL VARIABLE ϵ

Before proceeding to a discussion of specific conical solutions to the subsonic flow equations, it will be of interest to examine certain features of the conical variable

$$\epsilon = \frac{y + iz}{x + r} \quad .$$

Referring to Fig. 1, we have

$$|\epsilon| = \left| \frac{y^2 + z^2}{(x+r)^2} \right|^{\frac{1}{2}}$$

$$= \left| \frac{r - x}{r + x} \right|^{\frac{1}{2}}$$

$$= \tan \frac{\beta}{2} \quad ; \quad 0 \le \beta \le \pi$$

and

$$\arg \epsilon = \tan^{-1} \left(\frac{z}{y}\right) = \varphi \quad ; \quad 0 \le \varphi < 2\pi$$

Thus, considered as a mapping of the xyz space onto the $\epsilon = \xi + i\eta$ plane, half-rays emanating from the origin in the xyz space are mapped onto points in the ϵ plane. Furthermore, for each half-ray there exists a unique pair (β, φ) for which $0 \le \beta \le \pi$ and $0 \le \varphi < 2\pi$; and consequently, since $\tan \frac{\beta}{2}$ is single valued on this range, each half-ray is mapped onto a unique point in the ϵ plane. The inverse transformation

$$\beta = 2 \tan^{-1} |\epsilon| \qquad 0 \le \beta \le \pi$$

$$\varphi = \arg \epsilon \qquad 0 \le \varphi < 2\pi$$

is one-valued by the restricted ranges on β and φ and consequently for every point in the ϵ plane (including the point at infinity) there is a corresponding half-ray in the xyz space. Therefore the transformation is one-to-one in both directions in the sense that for each half-ray in xyz space there corresponds one and only one point in the ϵ plane, and conversely, for each point in the ϵ plane there corresponds one and only one half-ray in the xyz space. In particular it is noted (Fig. 2) that

(a) The plane $z = 0$ is mapped onto the real axis of ϵ .

(b) The plane $y = 0$ is mapped onto the imaginary axis of ϵ .

(c) The plane $x = 0$ is mapped onto the unit circle in the ϵ plane.

The one-to-one nature of the transformation allows, in the following, the treatment of the variable ϵ indiscriminately as representing either a point in the complex plane or a half-ray in the xyz space.

III. THE COMPATIBILITY RELATIONS

Suppose now that $U(\epsilon)$, $V(\epsilon)$, $W(\epsilon)$ are analytic functions of ϵ, and that they are separated into their real and imaginary parts as

$$\begin{aligned} U(\epsilon) &= u(\xi,\eta) + iu^*(\xi,\eta) \\ V(\epsilon) &= v(\xi,\eta) + iv^*(\xi,\eta) \\ W(\epsilon) &= w(\xi,\eta) + iw^*(\xi,\eta) \end{aligned}$$

Then by Eq. (1)

$$\nabla^2 u = \nabla^2 v = \nabla^2 w = 0,$$

where

$$\nabla^2 = \frac{\partial^2}{\partial x^2} + \frac{\partial^2}{\partial y^2} + \frac{\partial^2}{\partial z^2},$$

and we ask under what conditions (u,v,w) may be interpreted as the velocity components of a three-dimensional incompressible field. A necessary and sufficient condition for this is that

$$\begin{aligned} &\frac{\partial U}{\partial x} + \frac{\partial V}{\partial y} + \frac{\partial W}{\partial z} = 0 \\ &\frac{\partial U}{\partial y} = \frac{\partial V}{\partial x} \\ &\frac{\partial U}{\partial z} = \frac{\partial W}{\partial x} \\ &\frac{\partial V}{\partial z} = \frac{\partial W}{\partial y} \end{aligned} \qquad (2)$$

The real parts of these equations are the physical conditions of irrotationality and continuity. The necessity of Eq. (2) is due to the requirement of analyticity on U, V, and W, and may be shown by a direct application of the Cauchy-Riemann equations in the ϵ-plane to each of the complex velocity functions U, V, and W, separately.

Since $\nabla^2 U = \nabla^2 V = \nabla^2 W = 0$, and since the velocity functions are homogeneous of order zero, the first expression of Eq. (2) is satisfied if the last three are. Suppose then that

$$\frac{\partial U}{\partial y} = \frac{\partial V}{\partial x}$$

Then

$$\frac{dU}{d\epsilon}\,\frac{\partial \epsilon}{\partial y} = \frac{dV}{d\epsilon}\,\frac{\partial \epsilon}{\partial x}$$

but

$$\frac{\partial \epsilon}{\partial x} = -\frac{y + iz}{(x+r)^2}\left(1 + \frac{x}{r}\right) = -\frac{\epsilon}{r}$$

and

$$\frac{\partial \epsilon}{\partial y} = \frac{1}{x + r} - \frac{(y + iz)y}{(x+r)^2\, r}$$

$$= -\frac{1}{2r}\left[\frac{2(y^2 + iyz) - 2r(x + r)}{(x + r)^2}\right]$$

$$= -\frac{1}{2r}\left[\frac{(y^2 + 2\,iyz) - (r^2 - y^2) - (r^2 + 2rx)}{(x + r)^2}\right]$$

$$= -\frac{1}{2r}\left[\frac{y^2 + 2iyz) - (x^2 + z^2) - (r^2 + 2rx)}{(x + r)^2}\right]$$

$$= -\frac{1}{2r}\left[\frac{(y + iz)^2 - (x + r)^2}{(x + r)^2}\right]$$

$$= -\frac{\epsilon^2 - 1}{2r}$$

Therefore $\frac{\partial U}{\partial y} = \frac{\partial V}{\partial x}$ implies

$$\frac{(\epsilon^2 - 1)}{2}\,\frac{dU}{d\epsilon} = \epsilon\,\frac{dV}{d\epsilon}$$

or

$$\frac{dU}{d\epsilon} = \frac{2\epsilon}{\epsilon^2-1}\frac{dV}{d\epsilon}$$

Similarly, since

$$\frac{\partial \epsilon}{\partial z} = \frac{i}{x+r} - \frac{z(y+iz)}{r(x+r)^2}$$

$$= \frac{i}{2r}\left[\frac{2iz\,(y+iz) + 2r(x+v)}{(x+r)^2}\right]$$

$$= \frac{i}{2r}\left[\frac{(2iyz - z^2) + (r^2 - z^2) + (r^2 + 2xr)}{(x+r)^2}\right]$$

$$= \frac{i}{2r}\left[\frac{(2iyz - z^2) + (x^2 + y^2) + (r^2 - 2xr)}{(x+r)^2}\right]$$

$$= \frac{i}{2r}\left[\frac{(y+iz)^2 + (x+r)^2}{(x+r)^2}\right]$$

$$= \frac{i}{2r}\,(\epsilon^2 + 1)$$

the condition

$$\frac{\partial U}{\partial z} = \frac{\partial W}{\partial x}$$

implies

$$\frac{dU}{d\epsilon} = \frac{2i\epsilon}{\epsilon^2+1}\frac{dW}{d\epsilon}$$

and

$$\frac{\partial V}{\partial z} = \frac{\partial W}{\partial y}$$

implies

$$\frac{dV}{d\epsilon} = i\,\frac{\epsilon^2 - 1}{\epsilon^2 + 1}\frac{dW}{d\epsilon}$$

Since the derivatives $\frac{\partial \epsilon}{\partial x}, \frac{\partial \epsilon}{\partial y}, \frac{\partial \epsilon}{\partial z}$ are single valued the above

arguments may be inverted, and it may be concluded that a necessary and sufficient condition for the fulfillment of Eqs. (2) is that

$$\frac{dU}{d\epsilon} = \frac{2\,i\,\epsilon}{\epsilon^2 + 1}\,\frac{dW}{d\epsilon}$$

$$\frac{dU}{d\epsilon} = \frac{2\,\epsilon}{\epsilon^2 - 1}\,\frac{dV}{d\epsilon} \qquad (3)$$

These relations are referred to as the compatibility relations and they replace the irrotationality and continuity equations, Eqs. (2), for incompressible conical flow. By use of the Prandtl-Glauert transformation they may be used for linearized subsonic flow.

IV. SOURCE FIELDS

We now proceed to a discussion of a basic solution to Eq. (3) that may be interpreted as a particular distribution of sources in the xy plane. This basic solution is

$$U_1(\epsilon) = \frac{2w_o\ \epsilon_o}{\pi(\epsilon_o^2+1)} \log\left(\frac{\epsilon - \epsilon_o}{\epsilon + \frac{1}{\epsilon_o}}\right)$$

$$V_1(\epsilon) = \frac{w_o}{\pi}\left[\frac{\epsilon_o^2 - 1}{\epsilon_o^2 + 1} \log\left(\frac{\epsilon - \epsilon_o}{\epsilon + \frac{1}{\epsilon_o}}\right) + \log \epsilon\right] \qquad (4)$$

$$W_1(\epsilon) = -\frac{iw_o}{\pi} \log\left[\frac{(\epsilon + \frac{1}{\epsilon_o})(\epsilon - \epsilon_o)}{\epsilon}\right]$$

where ϵ_o and w_o are positive real constants. The associated real velocity field is

$$u_1 = \mathrm{Rl}\,(U_1) = \frac{2w_o\ \epsilon_o}{\pi(\epsilon_o^2 + 1)} \log\left|\frac{\epsilon - \epsilon_o}{\epsilon + \frac{1}{\epsilon_o}}\right|$$

$$v_1 = \mathrm{Rl}\,(V_1) = \frac{w_o}{\pi}\left[\frac{\epsilon_o^2 - 1}{\epsilon_o^2 + 1} \log\left|\frac{\epsilon - \epsilon_o}{\epsilon + \frac{1}{\epsilon_o}}\right| + \log|\epsilon|\right] \qquad (4a)$$

$$w_1 = \mathrm{Rl}\,(W_1) = \frac{w_o}{\pi} \arg\frac{(\epsilon + \frac{1}{\epsilon_o})(\epsilon - \epsilon_o)}{\epsilon}$$

In order to make w_1 single-valued, the ϵ plane is cut as shown in Fig. 3a. The corresponding cuts in x,y,z space are shown in Fig. 4. Since u_1 and v_1 are single valued, it is not necessary to construct a specific cut system for U_1 and V_1, however, a convenient system of cuts for these two functions is shown in Fig. 3b. These cuts are not significant in the real velocity field and are deleted from Fig. 4 for clarity. Use has been made of the general relation

$$\frac{1}{\epsilon(x,y,z)} = -\epsilon(-x,-y,z)$$

so that the half-ray $\epsilon = -\frac{1}{\epsilon_o}$ is the extension through the origin of the half-ray $\epsilon = \epsilon_o$.

If ϵ is made to approach a point on the cut to the right of the origin from above, it is seen from the expression for w in Eq. (4a) that

$$\lim_{\substack{\epsilon \to \xi + i0 \\ 0 < \xi < \epsilon_o}} w = w_o$$

whereas if approached from below

$$\lim_{\substack{\epsilon \to \xi - i0 \\ 0 < \xi < \epsilon_o}} w = -w_o$$

The same values of w occur on the cut to the left of $-\frac{1}{\epsilon_o}$, and elsewhere on the ξ axis w has the value zero.

The field of Eq. (4a) is then the field associated with a uniform source sheet of strength w_o distributed over a double-sector in the xy plane. This field is represented schematically in Fig. 5, where the values of w are shown in the xy plane, approached from above.

We shall refer to this particular field symbolically as $F_1(x,y,z;\epsilon_o)$, where F_1 may be thought of as a complex vector with components (U,V,W).

Formally, fields of the type $F_1(x,y,z;\epsilon_o)$ may be superimposed to produce fields of finite extent. Such a superposition is one which gives a triangular source-sheet and may be expressed as

$$G_1(x,y,z;\epsilon_o,c) = \tfrac{1}{2}\Big[F_1(x,y,z;\epsilon_o) - F_1(x-c,y-b,z;\epsilon_o) + F_1(x-c,y-b,z;1) - F_1(x-c,y,z;1)\Big] \qquad (5)$$

where c is a real positive constant and

$$b = \frac{2\epsilon_o c}{1-\epsilon_o^2}$$

This superposition is shown graphically in Fig. 6, where the values of w in the xy plane, approached from above, are given for the component fields and the resultant field. The values of w on the xy plane approached from below are the negative of those shown.

It should be noted that b as defined above may be either positive or negative, depending on the magnitude of ϵ_o, and in particular, $-G_1(x,y,z;\frac{1}{\epsilon_o}, c)$ is the reflection of $G_1(x,y,z;\epsilon_o,c)$ across the x-axis.

The question is raised at this point as to whether such a superposition is proper, since the function $G(x,y,z;\epsilon_o, c)$ is not strictly defined along the half-rays associated with the singularities of the conical field F_1. (These half-rays are indicated by the dashed lines of Fig. 6e.) Certain general statements will be made with respect to this question in the following section.

V. SUPERPOSITION OF CONICAL FIELDS

The general requirement in superposing conical fields is the reduction of disturbances of infinite extent to disturbances of finite extent. The procedure, as indicated in the formal superposition above, is to superpose identical conical fields in pairs, one of the pair being displaced, in xyz space, from the other along a half-ray that is a singularity of the particular conical field. Thus the first two conical fields in the superposition above (a and b of Fig. 6) are identical, the second one (b) being displaced from the first along the singular half-ray $\epsilon = \epsilon_0$, and the superposition is a subtractive one.

Consider now a conical field $F(x,y,z) = f(\epsilon)$ say, and suppose it is desired to superimpose this field on itself by the procedure indicated above. For convenience, we shall suppose that the xyz axes are oriented so that the singular half-ray in which we are interested lies along the negative x axis, corresponding to $\epsilon = \infty$. The superposition may then be expressed as

$$G(x,y,;c) = F(x,y,z) - F(x - c,y,z) \tag{6}$$

or equivalently

$$g(\epsilon\ ;\varsigma) = f(\epsilon) - f(\varsigma)$$

where

$$\varsigma(x,y,z) = \epsilon(x - c,y,z)$$

$$= \frac{y + iz}{x-c + \sqrt{(x-c)^2 + y^2 + z^2}} \quad ,$$

and the notation $g(\epsilon\ ;\varsigma)$ is used to emphasize the fact that ϵ and ς are not independent variables, their values being uniquely determined

by the specification of the variables (x,y,z) and the parameter c.

The geometry associated with this superposition is shown in Fig. 7, and it is seen that the half-rays ϵ and ς intersect at the point (x,y,z), the ϵ ray emanating from the origin (0,0,0) and the ς ray emanating from the point (c,0,0). Now suppose that the point (x,y,z) is not on the x axis and that the value of ϵ is fixed. If the point (x,y,z) is allowed to move out on the ϵ ray, ς will vary continuously, and it is clear from the geometry that

$$\lim_{\substack{r \to \infty \\ \epsilon = \text{constant}}} \varsigma = \epsilon$$

If the point (x,y,z) is on the x axis, there are three possibilities:

for y = z = 0:

1. $x > c$ we have $\epsilon = \varsigma = 0$; all $x > c$
2. $0 < x < c$ we have $\epsilon = 0$ and $\varsigma = \infty$; all x, $0 < x < c$
3. $x < 0$ we have $\epsilon = \varsigma = \infty$; all $x < 0$

It should be noted in connection with the third possibility, however, that

$$\lim_{\substack{y,z \to 0 \\ x < 0}} (\epsilon - \varsigma)$$

does not exist, for, letting $p = \sqrt{y^2 + z^2} \geq 0$;

$$\lim_{\substack{y,z \to 0 \\ x < 0}} \left[|\epsilon^n| - |\varsigma^n| \right] = \lim_{\substack{p \to 0 \\ x < 0}} \left[\left(\frac{p}{\sqrt{x^2+p^2} - |x|} \right)^n - \left(\frac{p}{\sqrt{(x-c)^2+p^2} - |x-c|} \right)^n \right]$$

$$= \lim_{\substack{p \to 0 \\ x < 0}} p^n \left[\left(\frac{\sqrt{x^2+p^2} + |x|}{p^2} \right)^n - \left(\frac{\sqrt{(x-c)^2 + p^2} + |x-c|}{p^2} \right)^n \right]$$

$$= \lim_{\substack{p \to 0 \\ x < 0}} \frac{1}{p^n} \left[\left(\sqrt{x^2+p^2} + |x| \right)^n - \left(\sqrt{(x-c)^2 + p^2} + |x-c| \right)^n \right]$$

and this limit does not exist for $n > 0$. For $n \leq 0$, however, the limit does exist and is zero.

It is also of interest to note, in connection with the three possibilities above, that

1a. for $x > c$

$$\lim_{p \to 0} (\epsilon/\zeta) = \lim_{p \to 0} \left(\frac{\sqrt{(x-c)^2 + p^2} + (x-c)}{\sqrt{x^2+p^2} + x} \right)$$

$$= \frac{x-c}{x}, \quad x > c$$

2a. for $0 < x < c$

$$\lim_{p \to 0} (\epsilon/\zeta) = 0$$

3a. for $x < 0$

$$\lim_{p \to 0} (\epsilon/\zeta) = \lim_{p \to 0} \left(\frac{\sqrt{(x-c)^2 + p^2} - |x-c|}{\sqrt{x^2+p^2} - |x|} \right)$$

$$= \lim_{p \to 0} \left(\frac{\sqrt{x^2 + p^2}}{\sqrt{(x-c)^2 + p}} \right) \text{ by L'Hospital's rule}$$

$$= \frac{x}{x-c}, \quad x < 0$$

Returning to the fields F and G of Eq. (5) it is seen, as a consequence of the geometrical properties discussed above, that if ϵ is a point of regularity of $f(\epsilon)$, then

$$\lim_{\substack{r \to \infty \\ \epsilon = \text{const.}}} G(x,y,z;c) = \lim_{\zeta \to \epsilon} \left(f(\epsilon) - f(\zeta) \right) = 0$$

For the particular case where (x,y,z) is on the x axis, the value of G is defined as

$$G(x,0,0;c) = \lim_{p \to 0} \left(F(x,y,z) - F(x-c,y,z) \right)$$

where this limit exists.

It was assumed to begin with that $F(x,y,z)$ was singular on the negative x axis ($\epsilon = \infty$); and since

$$\lim_{\substack{p \to 0 \\ x < 0}} (\epsilon^n - \zeta^n) \qquad n > 0$$

does not exist, $G(x,0,0;c)$ will not exist if the singularity of F on the negative x axis is in the nature of a pole or an isolated essential singularity of $f(\epsilon)$ at $\epsilon = \infty$.

On the other hand if $f(\epsilon)$ has a branch point at $\epsilon = \infty$ such that $f(\infty)$ can be made to exist by introducing suitable cuts, or if $f(\epsilon)$ has a logarithmic singularity at $\epsilon = \infty$, then $G(x,0,0;c)$ will exist for $x < 0$, provided that the proper cuts are introduced.

The case of a logarithmic singularity is of particular interest and if we put

$$f(\epsilon) = A \log \epsilon + f_1(\epsilon)$$

where $f_1(\epsilon)$ is regular at $\epsilon = \infty$ and the ϵ plane is assumed cut to

$\epsilon = \infty$, along the real axis, say, then for $x < 0$

$$G(x,0,0;c) = \lim_{\substack{p \to 0 \\ x < 0}} A \log \left(\frac{\epsilon}{\zeta} \right) + \lim_{\substack{\zeta \to \epsilon \\ \epsilon \to \infty}} \left(f_1(\epsilon) - f_1(\zeta) \right)$$

$$= A \log \left(\frac{x}{x-c} \right); \quad x < 0$$

Consequently $G(x,0,0;c)$ does exist on the negative x axis even though the component conical fields are singular there.

The above discussion was carried out for the case of a singularity along the negative x axis, however the results are quite general and may be applied to any other half-ray since any half-ray may be made to coincide with the negative x axis by a simple rotation of the space.

It is to be noted that, in the example given above, G is singular on the segment $0 < x < c$ which corresponds to $\epsilon = 0$ and $\zeta = \infty$. This result is general and the effect of superpositions of the type discussed is to cancel all but a finite segment of the singular half-ray of the conical field F.

A simple construction serves to illustrate the character of a field obtained by superposing singularities which are poles in the ϵ plane.

Consider a conical field in which one of the velocity functions, W say, is given by

$$W_o(\epsilon) = - ia \log \left(\frac{\epsilon - \delta}{\epsilon} \right)$$

with δ real and positive. Then

$$\lim_{\substack{\delta \to 0 \\ a\delta = \text{constant}}} W_o = i \lim_{\substack{\delta \to 0 \\ a\delta = k}} \left(\frac{a\delta}{\epsilon} + \theta(\delta) \right) = \frac{ik}{\epsilon}$$

Now consider the superposition

$$W_1(x,y,z;c) = W_o(\epsilon) - W_o(\varsigma)$$

This superposition is shown in Fig. 8, which is a uniform source sheet of width h. The limit

$$\lim_{\substack{\delta \to 0 \\ a\delta = k}} W_1 = ik\left(\frac{1}{\epsilon} - \frac{1}{\varsigma} \right)$$

is the same field as that obtained by

$$\lim_{\substack{\sigma \to 0 \\ ah = \text{constant}}} W_1 \quad \text{where} \quad \sigma = 2 \tan^{-1} \delta$$

since for small δ

$$\delta = \tan \frac{\sigma}{2} \approx \frac{\sigma}{2}$$

and $h \approx \sigma c \approx 2\delta c$

The resulting downwash field is thus obtained by the coalescing of the edges of a source-sheet in the manner shown, at the same time keeping the total flux (corresponding to ah) fixed, and the result is a semi-infinite source whose strength is a function of x, increasing linearly from zero at x = 0 to the value ah at x = c and constant for x > c. In particular the resulting disturbance does not die out for large values of x.

As indicated previously, this result is characteristic of superposition of poles of any order, and consequently conical fields in which any of the velocity functions have poles can not be superposed to obtain fields in which disturbances die out at large distances from a body.

Since in general a given conical field will have more than one singularity, several superpositions must be made in order to provide proper cancellation of all singularities; however, the linear nature of the process permits the superposition to be carried out in any order.

As an example, consider the field $F_1(x,y,z;\epsilon_o)$ of Eq. (4) and the superposition indicated by Eq. (5) and Fig. 6: Since the field F_1 possesses only logarithmic singularities, it qualifies for superposition by the procedure outlined above. Referring to Fig. 6, it is seen that the combination of (a) and (b) provides proper cancellation along the singularity $\epsilon = \epsilon_o$, (a) and (d) provides proper cancellation along the x axis, (b) and (c) provides proper cancellation along the line $y = b$, and (c) and (d) provides proper cancellation along the line $x = c$. Thus the resultant field (e) is non singular except on the boundaries of the triangle, and the resultant velocities (u,v,w) become arbitrarily small at large distances from the triangle.

VI. NON-LIFTING THIN WINGS

The conical field $F_1(x,y,z;\epsilon_o)$, Eq. (4), and superpositions of the type $G_1(x,y,z;\epsilon_o,c)$ of Eq. (5) may be used to construct fields associated with a particular class of physically interesting bodies. They are symmetrical wings at zero angle of attack whose maximum thickness is small enough that the boundary conditions on the surface of the wing may be replaced by boundary conditions in the chord-plane of the wing.

Although an infinite superposition, or integration, of such fields may be used, in principle, to obtain the field associated with a thin wing of arbitrary planform and thickness distribution, the technique is particularly suitable for determining the flow about thin wings of polygonal planform and airfoil section, such as are common in much of present day supersonic wing design. The subsonic characteristics of such wings are important, since invariably these wings must accelerate through the subsonic regime before attaining supersonic speeds.

To illustrate the technique, consider the superposition

$$
\begin{aligned}
&G_2(x,y,z;\epsilon_o,\epsilon_2,c) \\
&= G_1(x,y,z;\epsilon_o,c) - G_1\left(x,y,z;\frac{1}{\epsilon_o},c\right) \\
&\quad - 2G_1(x-c_1,y,z;\epsilon_1,c-c_1) + 2G_1\left(x-c_1,y,z;\frac{1}{\epsilon_1},c-c_1\right) \\
&\quad + G_1(x-c_2,y,z;\epsilon_2,c-c_2) - G_1\left(x-c_2,y,z;\frac{1}{\epsilon_2},c-c_2\right)
\end{aligned}
$$

where

$$0 < \epsilon_o < \epsilon_2 < 1$$

and

$$c_1 = \frac{c_2}{2} = \frac{1}{2}\left[1 - \frac{\epsilon_o(1-\epsilon_2)^2}{\epsilon_2(1-\epsilon_o^2)}\right]c$$

$$\epsilon_1 = \frac{b}{(c-c_1) + \sqrt{b^2 + (c-c_1)^2}}$$

$$b = \frac{2\epsilon_o \; c}{1 - \epsilon_o^2}$$

This superposition is shown graphically in Fig. 9, and it is seen that the resulting planform is that of a symmetrical delta wing with a re-entrant trailing edge, and that the values of w on the surface are those associated with the perturbation field of a thin double-wedge airfoil section with a leading edge half-angle equal to $\frac{w_o}{q}$ where q is the free stream velocity. The real velocity components of the field G_2 are therefore the perturbation velocities due to this delta-wing, and in particular the x-component, u(x,y,z) evaluated on the wing is proportional to the pressure on the wing, according to the general linearized wing theory.

Since the field for this wing was determined solely by superpositions of the conical field $F_1(x,y,z;\epsilon_o)$, given in Eq. (4), the pressure on the surface, in any actual case, may be computed by superimposing values of u_1 calculated from Eq. (4a).

As another example, consider the field

$$G_3(x,y,z;\epsilon_o,c_1,c_2) = \tfrac{1}{2}\Big[F_1(x,y,z;\epsilon_o) - F_1(x-c_1,y-b,z;\epsilon_o) - F_1(x-c_2,y,z;\epsilon_o) + F_1(x-c_1-c_2,y-b,z;\epsilon_o)\Big] \tag{7}$$

where, as before,

$$b = \frac{2\epsilon_o}{1 - \epsilon_o^2} \; c_1$$

and c_1, c_2, and ϵ_o are real positive constants.

This field, illustrated in Fig. 10, represents the flow past a swept thin wedge of finite chord and span, followed by a constant

thickness, infinite chord plate.

The reflection of this field across the x axis is given by

$$- G_3 \left(x,y,z; \frac{1}{\epsilon_o}, c_1, c_2\right)$$

and the superposition

$$G_4(x,y,z;\epsilon_o,c_1,c_2,c_3) = G_3(x,y,z;\epsilon_o,c_1,c_2) - G_3(x,y,z;\frac{1}{\epsilon_o},c_1,c_2)$$

$$- G_3(x-c_3,y,z;\epsilon_o,c_1,c_2) + G_3(x-c_3,y,z;\frac{1}{\epsilon_o},c_1,c_2$$

provides the perturbation field for a swept, constant chord wing with a modified double-wedge airfoil section (Fig. 11). As before, the pressure at any point on the surface may be calculated by a superposition of values of u_1 computed from Eq. (4a).

Values for the pressure coefficient along the mid-chord line and along the half-panel chord-line are plotted in Fig. 12 for the wing above, for the case

$$c_1 = 3\sqrt{3}, \; c_2 = \frac{3\sqrt{3}}{2} c_3 \quad \text{and} \quad \epsilon_o = \frac{1}{\sqrt{3}} .$$

This corresponds to a sweep angle of 30° and an aspect ratio of 6.

VII. VORTEX FIELDS -- CONSTANT PRESSURE WINGS

We now turn to a more interesting, however, much more complex, area; namely a discussion of lifting wings of zero thickness.

As in the non-lifting case, the boundary conditions on the flow will be linearized. That is, the angle of attack is assumed small enough to allow the boundary conditions on the wing itself to be satisfied in the plane of the wing (i.e., on the xy plane), and the pressure perturbations are assumed to vary linearly with the streamwise* velocity perturbation, u. As a consequence of these approximations, the streamwise velocity perturbation u must be an odd function of z, as shown by general linearized potential wing theory, and consequently u must be zero on z = 0 except on the wing itself, where it will be of the same magnitude on top of the wing and on the bottom, but of opposite sign.

A further consequence of the linearization of the boundary conditions is that the vorticity vector must lie in the xy plane and, since u = 0 off the wing, this implies that, off the wing,

$$\frac{\partial v}{\partial x} = 0 \quad \text{for} \quad z = 0$$

That is, the sidewash, v, in the wake is independent of x. If, then, v is a function only of the conical variable ϵ, we must have

$$\frac{\partial v}{\partial x} = \frac{dv}{d\epsilon} \cdot \frac{\partial \epsilon}{\partial x} = -\frac{\epsilon}{r}\frac{dv}{d\epsilon} = 0$$

on z = 0

---

* In this discussion, the wing will always be assumed to lie 'in' the xy plane and the streamwise direction will be assumed coincident with the positive x axis.

and consequently

$$\frac{dv}{d\epsilon} = 0$$

in the wake ($z = 0$).

The results above may be expressed in general as:

In any conical field, the wake due to a lifting surface has constant strength (vorticity) in both the spanwise and streamwise directions.

As a consequence of this, no finite superposition of conical fields can yield a flow in which the wake due to a lifting surface varies continuously in the spanwise direction.

The first of these statements leads to the interesting conclusion that the field associated with a lifting sector that possesses both a leading and a trailing edge (Fig. 13) is not conical. The reason for this is that the integral expression for the downwash, $w(x,y,z)$, obtained by applying the Biot-Savart law to the vorticity field illustrated, does not converge. Attempts to describe such a field with conical variables result in the appearance of singularities elsewhere in the flow, and it is this fact which led Lampert[3] to the erroneous results mentioned earlier.

We now consider superpositions of conical fields which may be used to approximate the real fields which were ruled out above.

Consider first the conical field $F_2(x,y,z;\epsilon_o)$ defined by

$$U_2 = -\frac{iu_o}{\pi} \log \frac{\epsilon - \epsilon_o}{\epsilon + \epsilon_o}$$

$$V_2 = -\frac{iu_o}{2\pi\,\epsilon_o}\left[(\epsilon_o^2 - 1)\log(\epsilon^2 - \epsilon_o^2) + 2\log\epsilon\right]$$

$$W_2 = -\frac{u_o}{2\pi\,\epsilon_o}\left[(\epsilon_o^2 + 1)\log(\epsilon^2 - \epsilon_o^2) - 2\log\epsilon\right]$$

where ϵ_o is a real constant, $0 < \epsilon_o < 1$, u_o is a real positive constant, and the ϵ-plane is cut from $\epsilon = \epsilon_o$ to the left through real negative values of ϵ to ∞. The logarithm is assumed to have its principal value, with its value being assumed on the cut approached from above.

The real velocity components are

$$u_2 = \frac{u_o}{\pi}\arg\left(\frac{\epsilon - \epsilon_o}{\epsilon + \epsilon_o}\right)$$

$$v_2 = \frac{u_o}{2\pi\,\epsilon_o}\left[(\epsilon_o^2 - 1)\arg(\epsilon^2 - \epsilon_o^2) + 2\arg\epsilon\right]$$

$$w_2 = -\frac{u_o}{2\pi\,\epsilon_o}\left[(\epsilon_o^2 + 1)\log|\epsilon^2 - \epsilon_o^2| - \log|\epsilon|\right]$$

This field was discussed by Lampert and consists of vortex-sheets in the xy plane as illustrated in Fig. 14, where the values of u and v shown are those on the xy plane approached from above.

The superposition

$$G_5(x,y,z;\,\epsilon_o,c) = F_2(x,y,z;\,\epsilon_o) - F_2(x-c,y,z;\,\epsilon_o)$$

yields the perturbation field for an infinite span swept wing with constant pressure everywhere on the surface (Fig. 15). The reader is referred to Lampert's paper for a discussion of the camber distribution associated with this wing.

In order to construct finite-span wings, it is necessary to consider the field $F_3(x,y,z;\,\epsilon_o)$ defined by

$$U_3 = \frac{iu_o\,(1-\epsilon_o)}{\pi}\left[\log\left(\frac{\epsilon+1}{\epsilon-\epsilon_o}\right) + \frac{1+\epsilon_o}{1-\epsilon_o}\log\left(\frac{\epsilon-1}{\epsilon-\epsilon_o}\right)\right]$$

$$V_3 = -\frac{iu_o}{\pi}\,\frac{1-\epsilon_o^2}{\epsilon_o}\log\left(\frac{\epsilon}{\epsilon-\epsilon_o}\right)$$

$$W_3 = \frac{u_o\,(1-\epsilon_o^2)}{\pi\,\epsilon_o}\left[\log\left(\frac{\epsilon}{\epsilon-\epsilon_o}\right) + \frac{\epsilon_o}{1-\epsilon_o^2}\log\left(\frac{\epsilon-1}{\epsilon+1}\right) + \frac{\epsilon_o^2}{1-\epsilon_o^2}\log\left(\frac{\epsilon^2-1}{[\epsilon-\epsilon_o]^2}\right)\right] \quad ; 0 < \epsilon_o < 1$$

where the ϵ plane is cut on the real axis between $\epsilon = 1$ and $\epsilon = -1$.

This field consists of vortex sheets in the xy plane as shown in Fig. 16. The reflection of this field across the x axis is given by

$$-F_3(x,y,z;\,-\epsilon_o)$$

and is illustrated in Fig. 17.

The superposition

$$G_6(x,y,z;\,\epsilon_o,c) = F_3(x,y,z;\,\epsilon_o) - F_3(x-c,y-b,z;\,\epsilon_o)$$

where

$$b = \frac{\epsilon_o\,c}{1-\epsilon_o^2}$$

and c is a real positive constant, gives the field indicated in Fig. 18. The reflection of this field across the x axis is given by

$$-G_6(x,y,z;\,-\epsilon_o,c).$$

Now consider the superposition defined by

$$
\begin{aligned}
&G_7(x,y,z;\,\epsilon_o,c) \\
&= \tfrac{1}{2}\,G_6(x,y,z;\,\epsilon_o,c) \\
&\quad -\tfrac{1}{2}\,G_6(x,y,z;\,-\epsilon_o,c) \\
&\quad +\epsilon_o\,G_5(x,y,z;\,1,c).
\end{aligned}
\tag{9}
$$

This field is shown in Fig. 19 and is the perturbation field for a constant pressure delta wing. The surface shape necessary to support this pressure distribution is a highly cambered one and is characterized by logarithmic infinities in slope at the leading and trailing edges and along the centerline.

The reverse-delta constant pressure wing is obtained by the superposition

$$
\begin{aligned}
G_8(x,y,z;\,\epsilon_o,c) &= -\tfrac{1}{2}\,G_6(x,y+b,z;\,\epsilon_o,c) + \tfrac{1}{2}\,G_6(x,y+b;z;\,-\epsilon_o,c) \\
&\quad -\epsilon_o\,G_5(x,y,z;1,c)
\end{aligned}
\tag{10}
$$

where care must be taken to adhere to the strict definition of b as given in Eq. 8. This field is indicated in Fig. 20.

Since any polygonal planform which does not have streamwise tips (parallel to the x axis) can be partitioned into isosceles triangles like those of Figs. 19 and 20, these fields may be combined to obtain a constant pressure wing of such a planform. In such a superposition, the singularities in downwash in the component flows will cancel except on the boundaries of and downstream of the vertices of the resultant wing. A more interesting superposition of these fields is discussed in the next section.

VIII. APPROXIMATE SOLUTION TO THE FLAT PLATE WING

The concepts developed in the previous section may be applied to the construction of approximate models of real wings.

A technique using one such model is essentially due to Falkner[4,5] and consists of the following steps:

1. The velocity perturbation u on the wing is assumed to have a series expansion of the form

$$\begin{aligned}\frac{u(x,y)}{q\alpha} = \frac{4b}{c(\lambda)}\sqrt{1-\lambda^2}\Big[&(a_{00} + a_{02}\lambda^2 + a_{04}\lambda^4 + \ldots)\cot\frac{\theta}{2} \\ &+ (a_{10} + a_{12}\lambda^2 + a_{14}\lambda^4 + \ldots)\sin\theta \\ &+ (a_{20} + a_{22}\lambda^2 + a_{24}\lambda^4 + \ldots)\sin 2\theta \\ &+ \ldots\Big]\end{aligned} \tag{11}$$

where b is the wing semi-span,

$\lambda = \frac{y}{b}$,

$c(\lambda)$ is the wing chord at spanwise position $y = \lambda b$,

$\theta = \cos^{-1}\left(1 - \frac{2(x - x_\ell)}{c(\lambda)}\right)$,

$x - x_\ell$ is the chordwise coordinate of a point on the wing, measured from the leading edge.

This assumed form for u(x,y) is due to Blenk[6] and essentially represents

an expansion from the two-dimensional wing solution.

2. The above series is terminated so that a specified finite number of coefficients a_{ij} remain.

3. An approximate model of the wing is constructed which enables the determination of the coefficients a_{ij}.

The technique proposed here differs from that of Falkner in step 3.

Falkner's model (Fig. 21) consists of a finite set of finite strength horseshoe vortices distributed systematically over the wing planform. The lift due to each of these horseshoe vortices is distributed over a rectangular region in the neighborhood of the vortex and the resulting pressure is required to satisfy Eq. (11). This yields a linear relation between the unknown coefficients a_{ij} and the undetermined vortex strengths. The downwash at any point on the model of the wing is a linear function of the horseshoe vortex strengths and hence of the coefficients a_{ij}. The coefficients a_{ij} are then solved for by specifying the value of the downwash at as many points on the wing as there are unknowns a_{ij}.

One of the chief objections to the model of Falkner is the presence of concentrated vortices and the associated singularities in downwash on the wing.

The model proposed here is constructed by covering the wing planform with a finite number of the constant pressure triangles of Figs. 19 and 20. This model does not remove entirely the objectionable features of Falkner's model, but it does alleviate them somewhat in that the order of the down-wash singularities (logarithmic) is lower than in Falkner's case and as a result a more accurate determination of a given

number of the coefficients a_{ij} should result.

The procedure is as follows:

1. Terminate the series (Eq. 11) so that n coefficients a_{ij} remain.

2. Cover the wing planform with m triangles (Fig. 22) of the type of Figs. 19 and 20. Overlapping may occur in general, and for a curved planform the covering is only approximate.

3. Establish a pressure control point on each of the m triangles.

4. The pressure at each of these m control points is required to satisfy the terminated series, Eq. (11), giving an expression of the form

$$u_k = \sum_{\substack{i=1 \\ j=1}}^{i+j=n} a_{ij} f_{ij} (\theta_k, \lambda_k) \qquad k = 1,2,\ldots, m \qquad (12)$$

where the summation is over i and j, and (θ_k, λ_k) are the dimensionless coordinates of the k^{th} control point.

5. Pick an n-membered set of downwash control points and compute the downwash at each of these n points due to the m constant-pressure triangles, utilizing Eqs. (9) and (10). Note that due to the singularity on the x axis of Figs. 19 and 20, these points must not lie on the centerline of any of the triangles.

This gives

$$w_s = \sum_{k=1}^{m} h_{sk} u_k \qquad s = 1,2,\ldots, n \qquad (13)$$

where h_{sk} is the downwash at the s^{th} control point due to the k^{th} triangle with a unit value of u. Substituting Eq. (12) into Eq. (13) yields

$$w_s = \sum_{k=1}^{m} h_{sk} \sum_{\substack{i=1 \\ j=1}}^{i+j=n} a_{ij} f_{ij} (\theta_k, \lambda_k)$$

$$= \sum_{\substack{i=1 \\ j=1}}^{i+j=n} a_{ij} \sum_{k=1}^{m} h_{sk} f_{ij} (\theta_k, \lambda_k) \qquad (14)$$

$$= \sum_{\substack{i=1 \\ j=1}}^{i+j=n} A_{sij} a_{ij} \qquad s=1,2,\ldots,n$$

where

$$A_{sij} = \sum_{k=1}^{m} h_{sk} f_{ij} (\theta_k, \lambda_k)$$

Equation (14) represents an n^{th} order linear system in a_{ij} and w_s, and may be solved for the unknowns a_{ij} in terms of the specified downwash on the wing.

This technique was applied to the solution of a low-aspect ratio, flat delta wing and the results were generally unsatisfactory, difficulties being associated with the fact that the series (11) is not

directly applicable to the region downstream of the break in the leading edge.

Falkner was able to overcome this difficulty in his solutions by the application of somewhat arbitrary and semi-empirical modifications to the expression for u(x,y) and, although similar modifications could apparently be applied to the present technique, it was felt that the development of such procedures was beyond the scope of this work.

Another model may be constructed by approximating the planform of the given wing with a network of iscoceles triangles, as above, the pressure on each triangle being assumed constant but undetermined. The downwash field due to each constant pressure triangle is known from Eqs. (9) and (10) and consequently the total downwash at any point on the model may be expressed as

$$w(x_i, y_i) = \sum_{j=1}^{n} k_{ij} \quad u_j$$

where u_j is the streamwise perturbation velocity on the j^{th} triangle and h_{ij}, the influence coefficient, is the downwash at (x_i, y_i) due to the presence of the j^{th} triangle with unit streamwise perturbation velocity. Since h_{ij} is completely defined by either Eq. (9) or Eq. (10), a determinant system of linear algebraic equations is formed by specifying the value of downwash at n points (x_i, y_i) on the model:

$$w_i = \sum_{i=1}^{n} h_{ij} \quad u_j \qquad\qquad i = 1,2,\ldots,n$$

The solution of this system for u_j in terms of the specified values of w_i then yields an approximate pressure distribution for the wing.

Attempts to apply this method to a delta wing, using a 16 triangle network, were not successful, the chief difficulties apparently being associated with the use of too coarse a network and with the fact that for any finite n, the model is covered with a latticework of downwash singularities (the boundaries of each triangle and the lines emanating downstream from the vertices of each of the triangles). It is also to be noted that the Kutta condition is meaningless for such a technique since the requirement that the downwash be continuous at the trailing edge would be difficult to justify on a model which has singularities in downwash elsewhere on the wing.

A model is now suggested which does not have some of the objectionable features of those above. The basic element of the model is an isosceles triangle, as before, on which the pressure is allowed to vary linearly, with undetermined values (u_0, u_1, u_2) of streamwise perturbation velocity at each of the three vertices (Fig. 23). Such elements may be constructed by a suitable integration of the constant pressure triangles of Fig. 19 and Fig. 20. The wing planform is then covered by a network of such elements with the requirements that the pressure must be continuous within the boundaries of the wing, and must be zero at the trailing edge as prescribed by the Kutta condition. Such a model is shown in Fig. 24.

From preliminary investigation it appears that this model has the characteristic that the downwash field is continuous everywhere except at the leading edge and downstream of a break in the leading edge. It would seem therefore that treatment of this model is a manner similar to the second model mentioned above should yield a fair approximation

to the actual pressure distribution on a lifting wing. Since it was felt that this model represented a considerable deviation from the basic concept of conical flows, the matter was not investigated further.

REFERENCES

1. Donkin, W. F.: "Phil. Trans", (1857).

2. Jones, R. T.: "Subsonic Flow over Thin Oblique Airfoils at Zero Lift", N.A.C.A. Technical Note No. 1340, (1947).

3. Lampert, Seymour: "Conical Flow Methods Applied to Uniformly Loaded Wings in Subsonic Flow", Journal of the Aeronautical Sciences, Vol. 18, No. 2, p. 107, (1951).

4. Falkner, V. M.: "The Calculation of Aerodynamic Loading on Surfaces of any Shape", Aero. Research Council, R. & M., No. 1910, (1943).

5. Falkner, V. M.: "The Solution of Lifting Plane Problems by Vortex Lattice Theory", Aero. Research Council, R. & M., No. 2591, (1953).

6. Blenk, H.: "Der Eindecker als tragende Wirbelfläche", Z.A.M.M., Vol. 5, (1925).

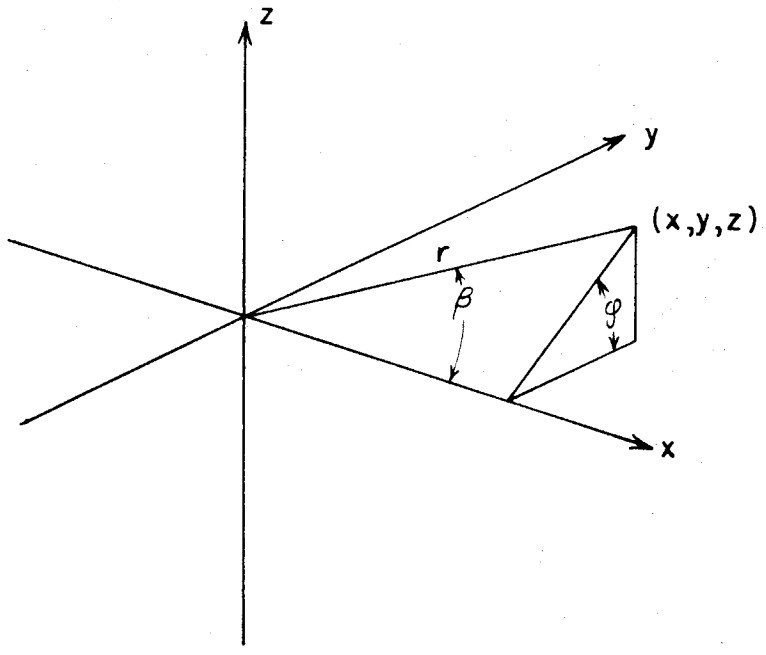

FIG. 1 - CONICAL REPRESENTATION OF X Y Z SPACE

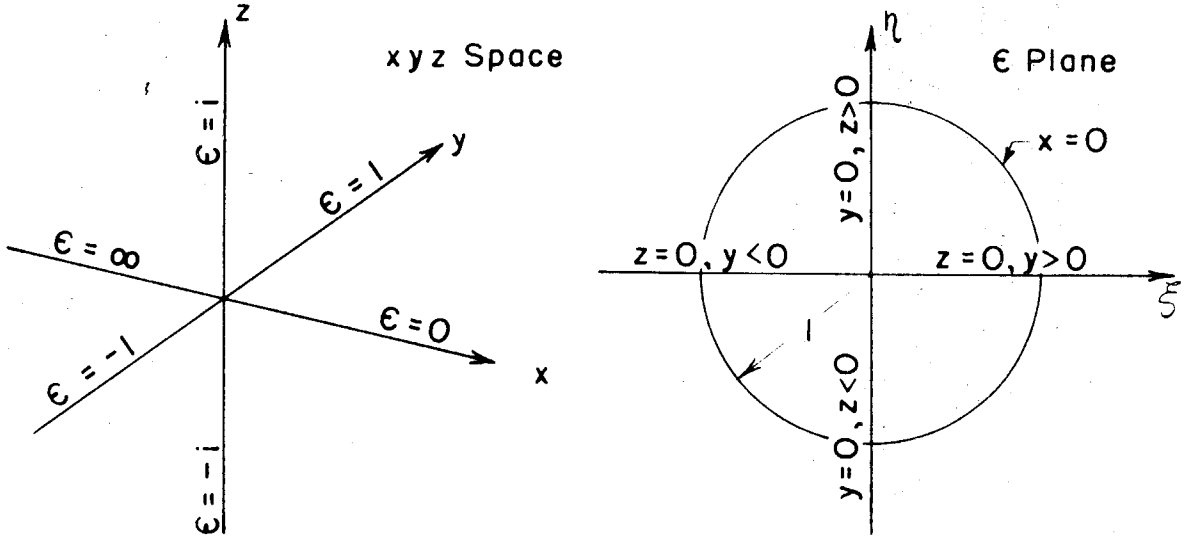

FIG. 2 - THE CONICAL MAPPING

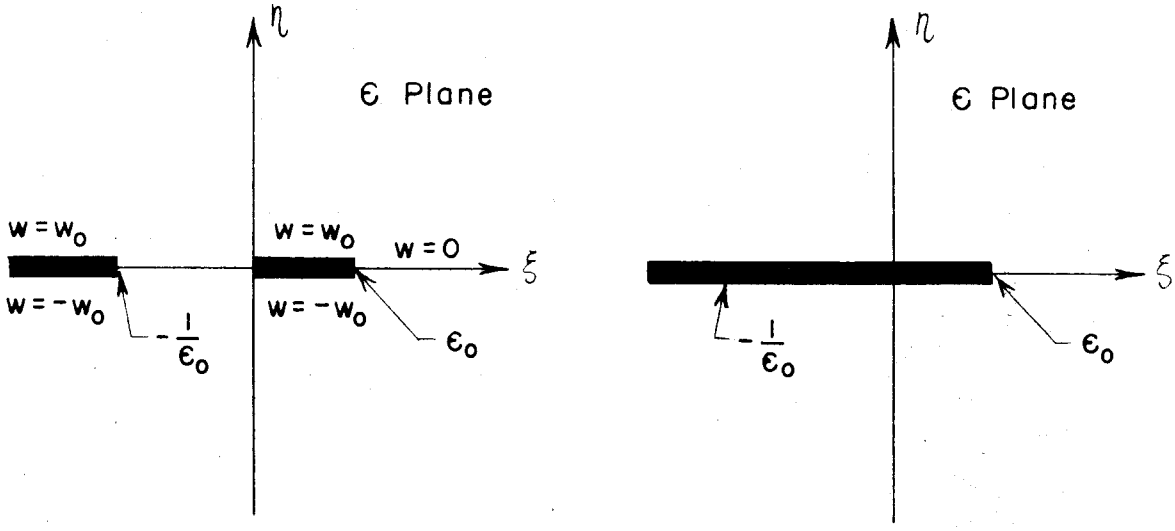

(a) Cut system for W_1 (b) Cut system for U_1 and V_1

FIG. 3 – REPRESENTATION OF $F_1(x,y,z;\epsilon_0)$ IN THE ϵ PLANE

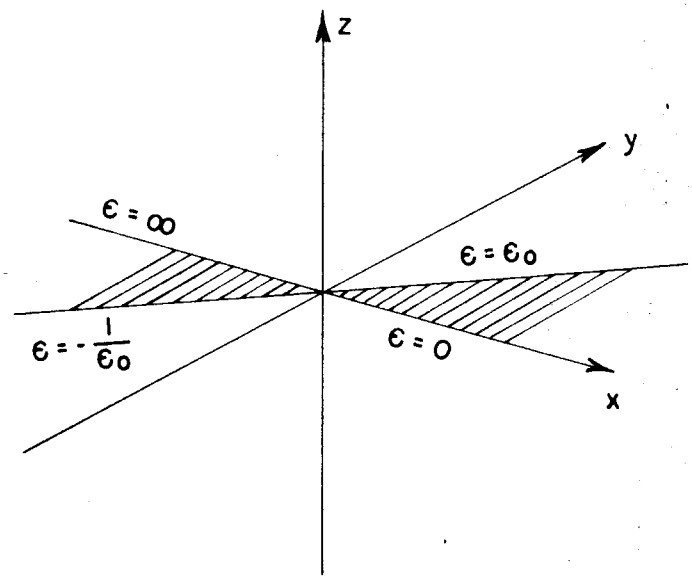

FIG. 4 – $F_1(x,y,z;\epsilon_0)$ IN xyz SPACE

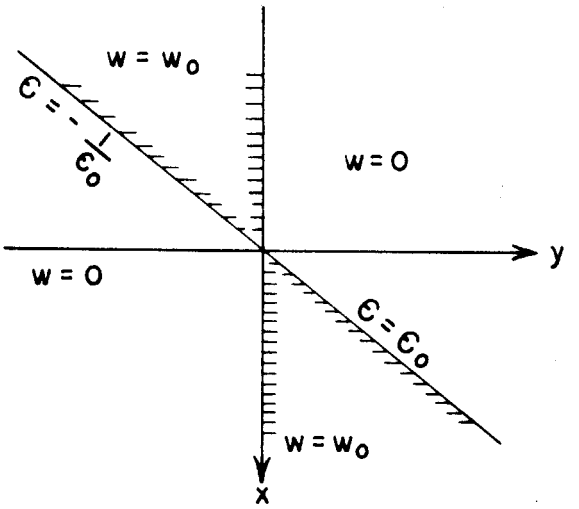

FIG. 5 – $F_1(x, y, z; \epsilon_0)$ IN THE xy PLANE

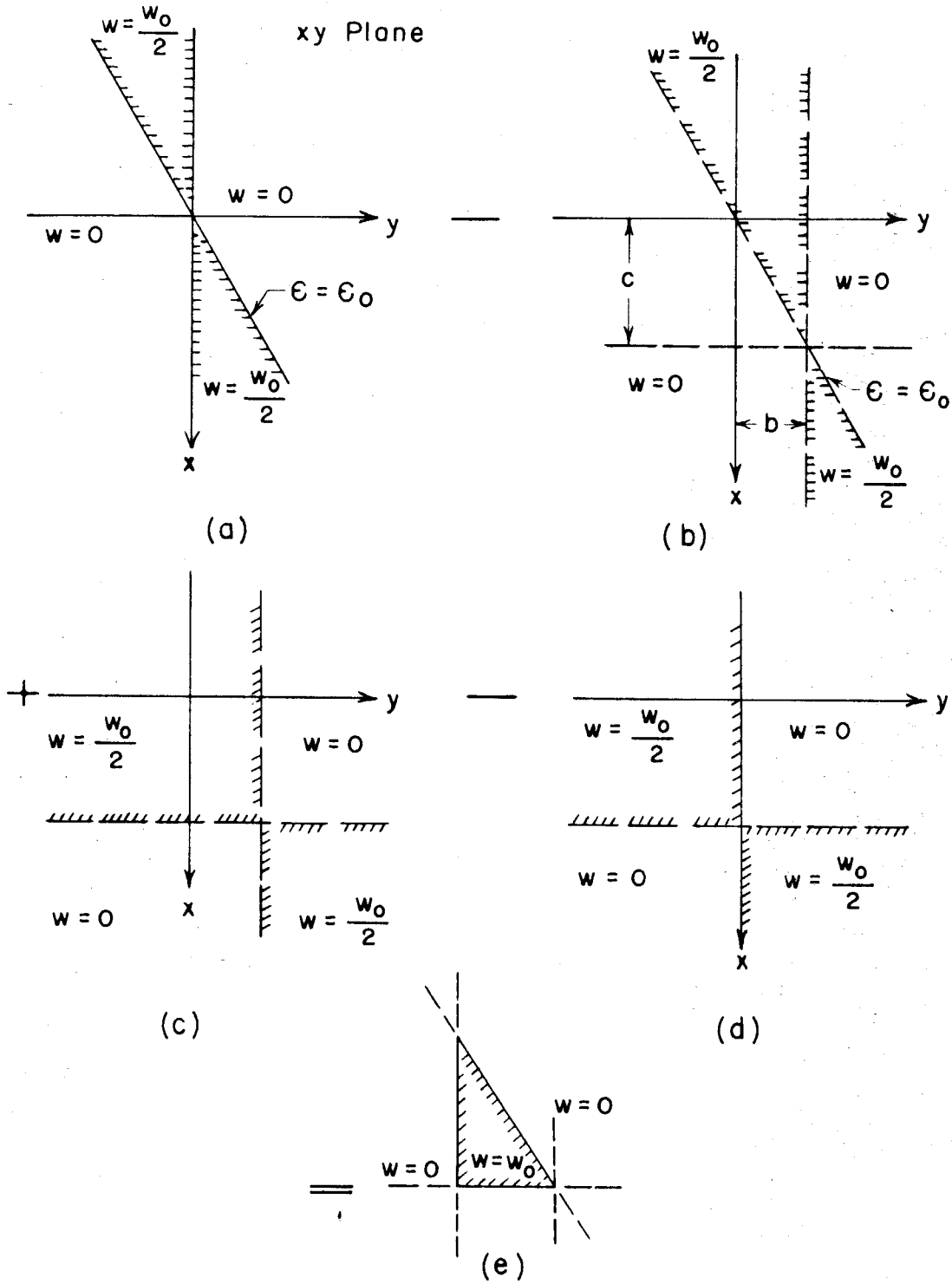

FIG. 6 — CONSTRUCTION OF A TRIANGULAR SOURCE SHEET

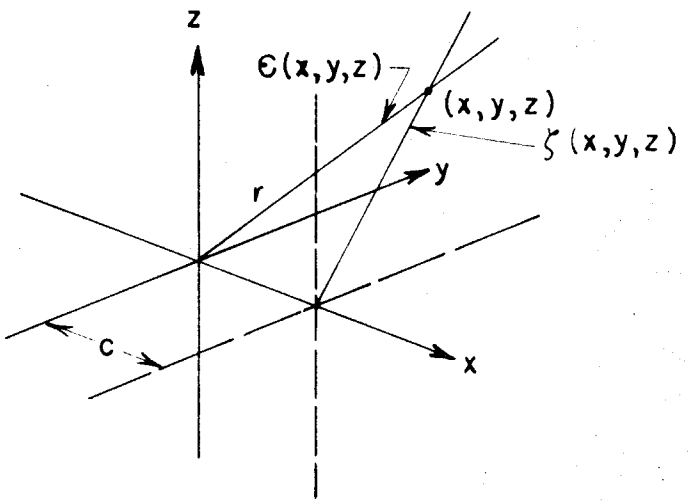

FIG. 7 – CONICAL SUPERPOSITION IN x y z SPACE

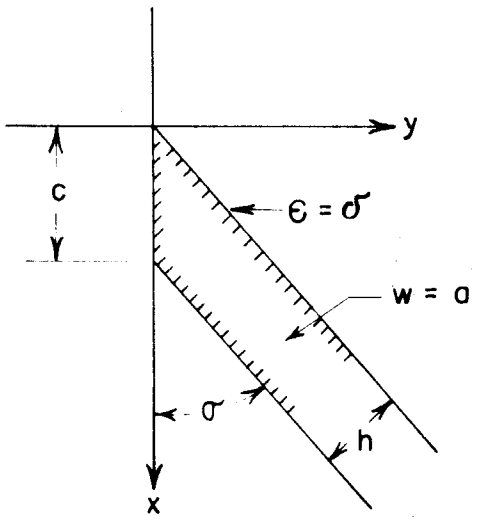

FIG. 8 – SEMI-INFINITE SOURCE SHEET

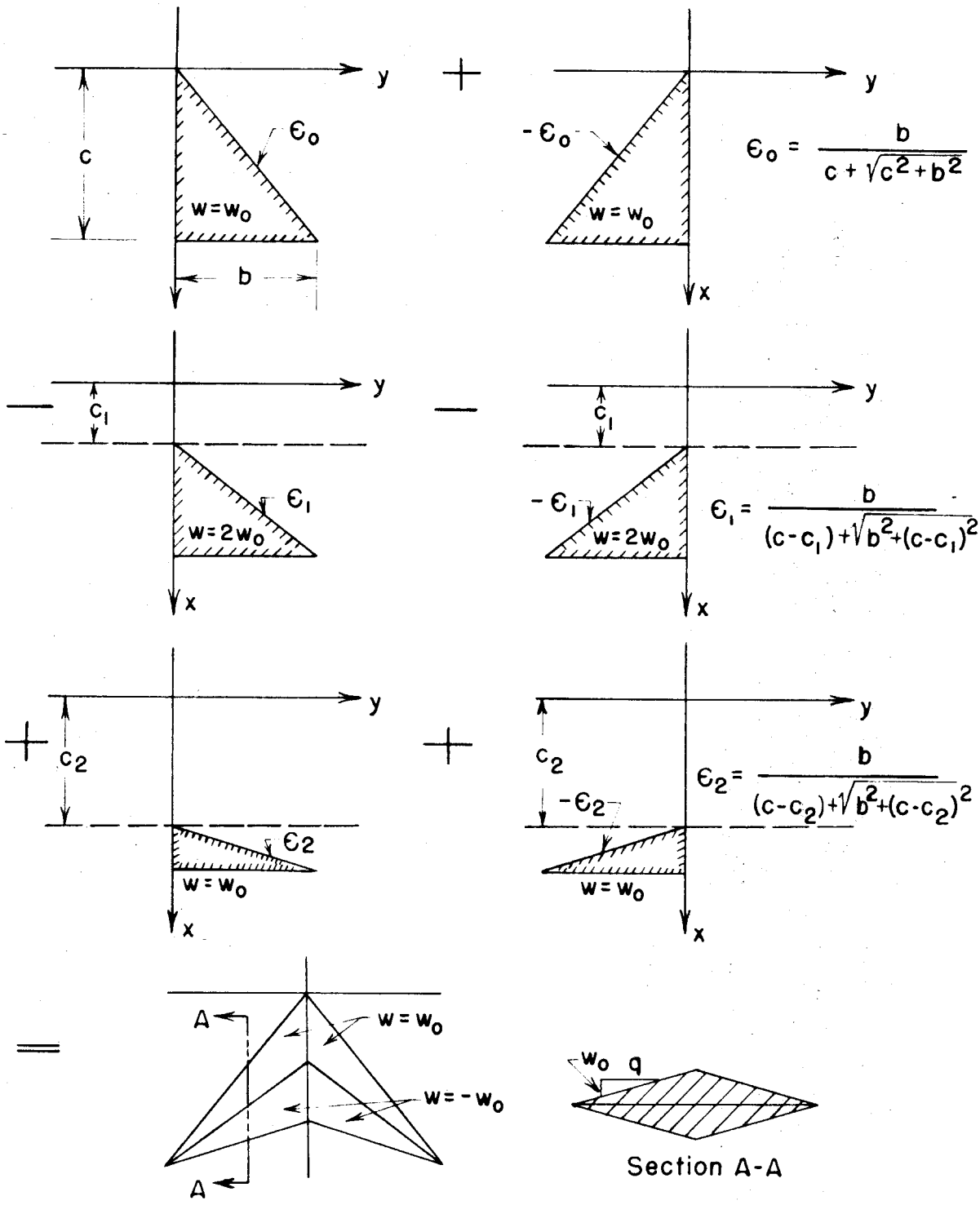

FIG. 9 – CONSTRUCTION OF A DOUBLE-WEDGE DELTA WING WITH RE-ENTRANT TRAILING EDGE

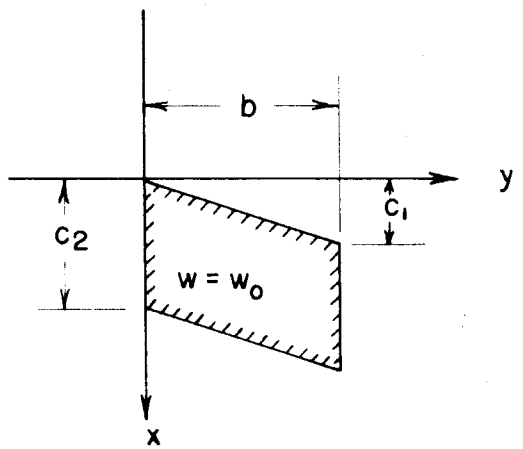

(a)

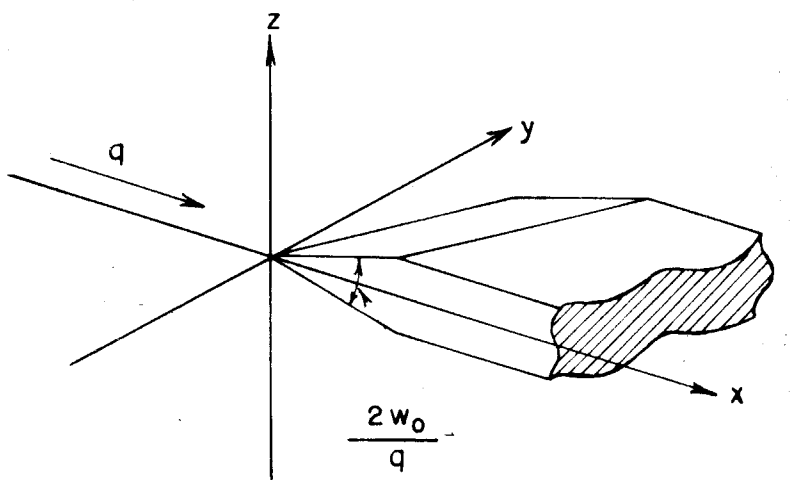

(b)

FIG. 10 – FINITE WEDGE

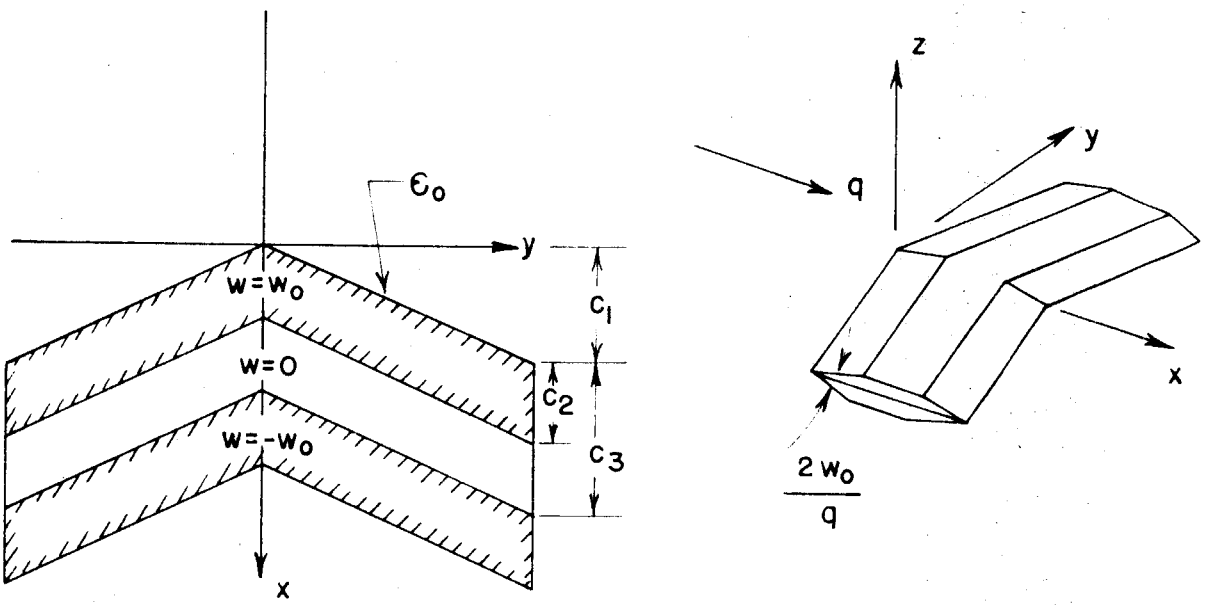

FIG. 11 – SWEPT WING WITH MODIFIED DOUBLE-WEDGE AIRFOIL SECTION

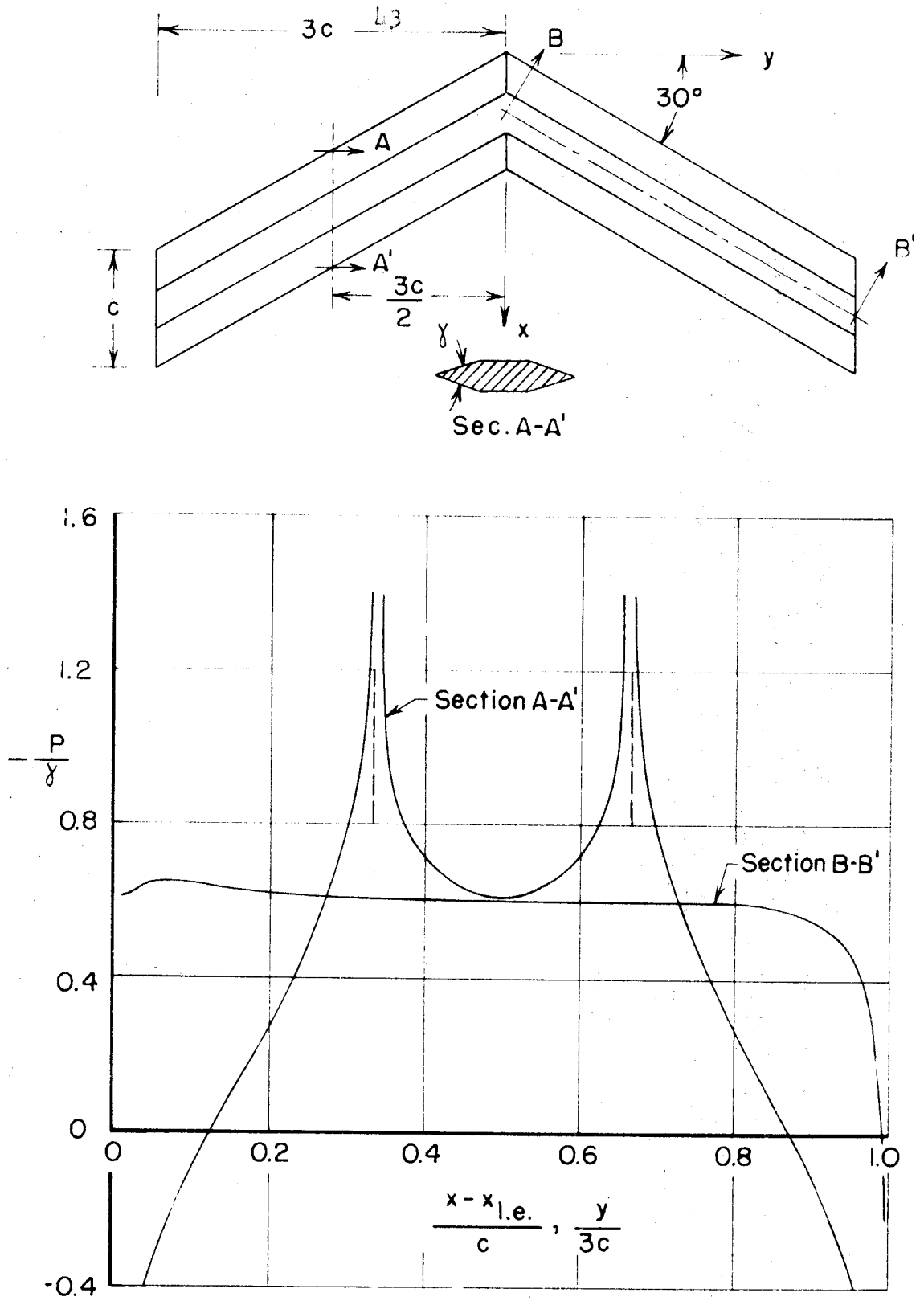

FIG. 12 – PRESSURE DISTRIBUTION AT ZERO LIFT ON A SWEPT WING WITH MODIFIED DOUBLE WEDGE AIRFOIL SECTION

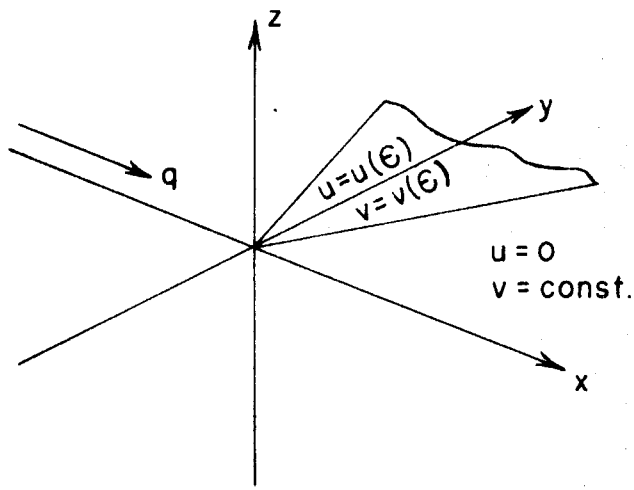

FIG. 13 – LIFTING INFINITE SECTOR

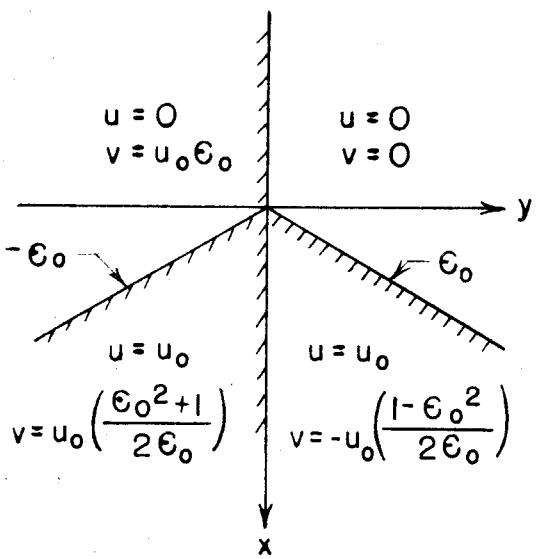

FIG. 14 – $F_2(x, y, z; \epsilon_0)$

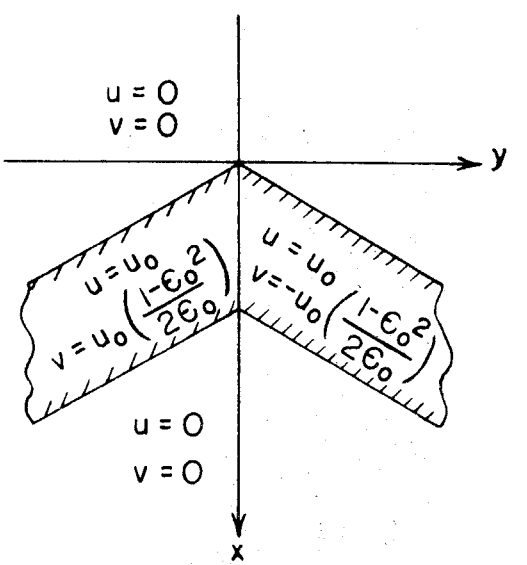

FIG. 15 – INFINITE SPAN CONSTANT PRESSURE SWEPT WING

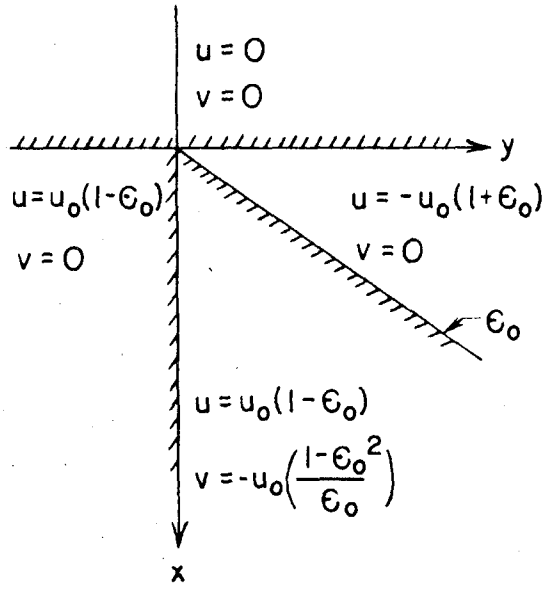

FIG. 16 – $F_3(x, y, z; \epsilon_0)$

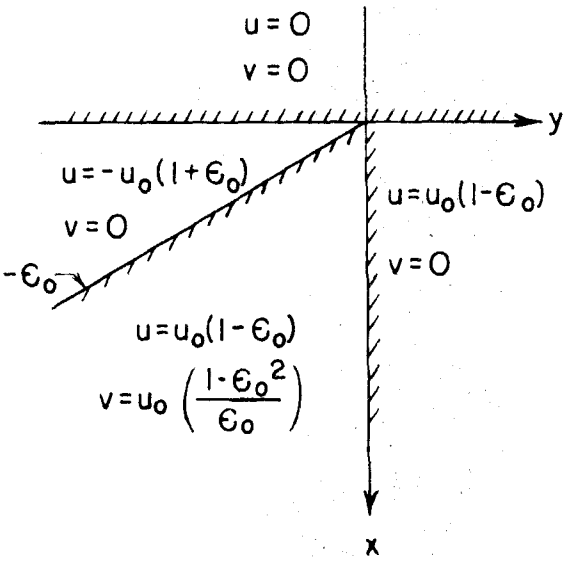

FIG. 17 – $-F_3(x, y, z; -\epsilon_0)$

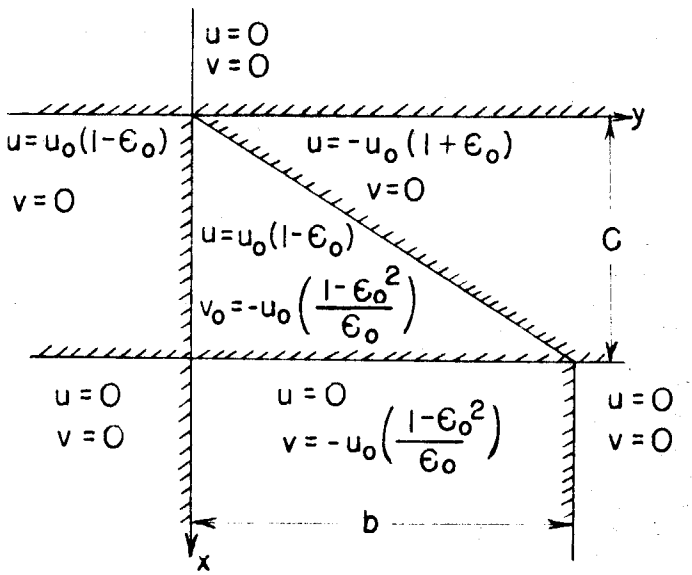

FIG. 18 – $G_6(x, y, z; \epsilon_0, C)$

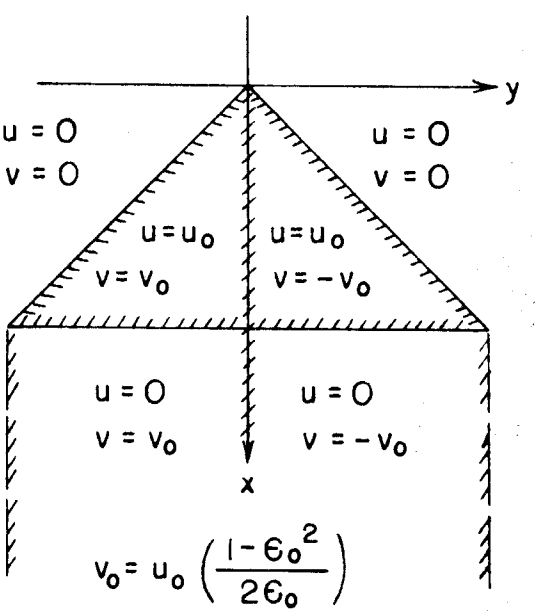

FIG. 19 - CONSTANT PRESSURE DELTA WING

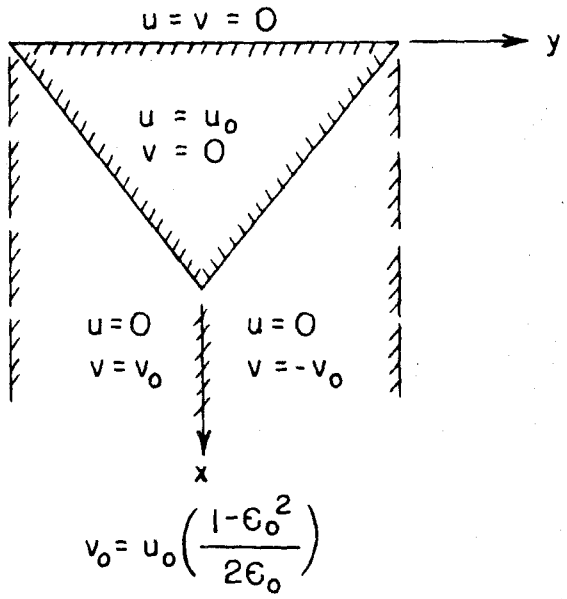

FIG. 20 — CONSTANT PRESSURE REVERSE DELTA WING

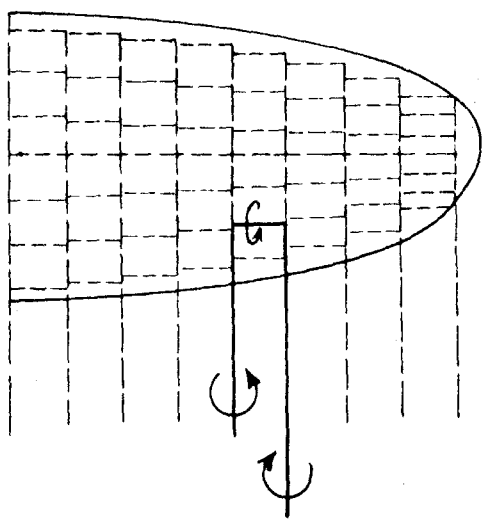

FIG. 21 — FALKNER'S HORSESHOE VORTEX MODEL

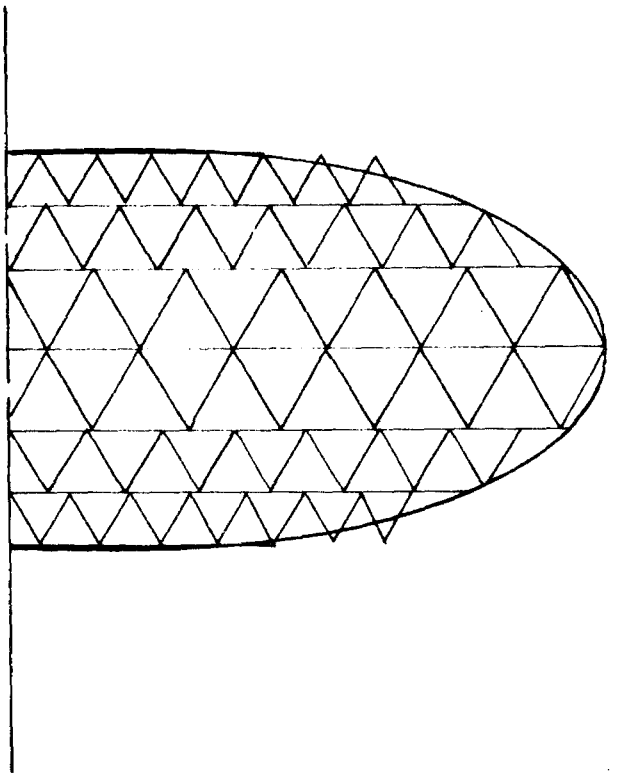

FIG. 22 - CONSTANT PRESSURE TRIANGLE MODEL

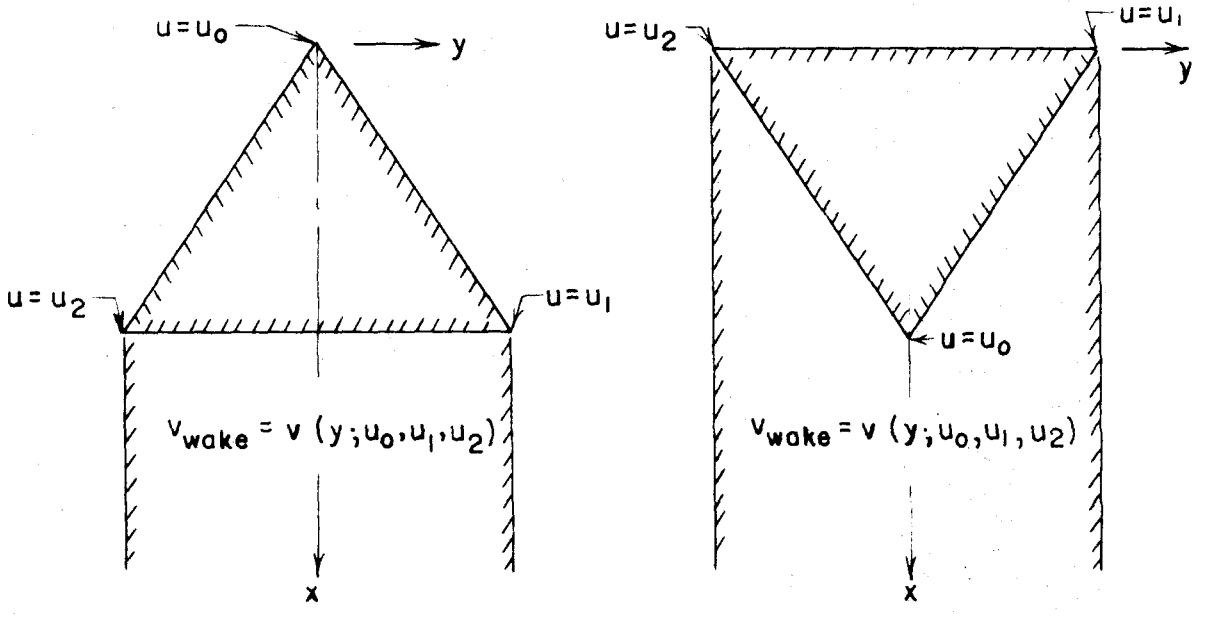

FIG. 23—TRIANGULAR WINGS WITH LINEAR PRESSURE DISTRIBUTION

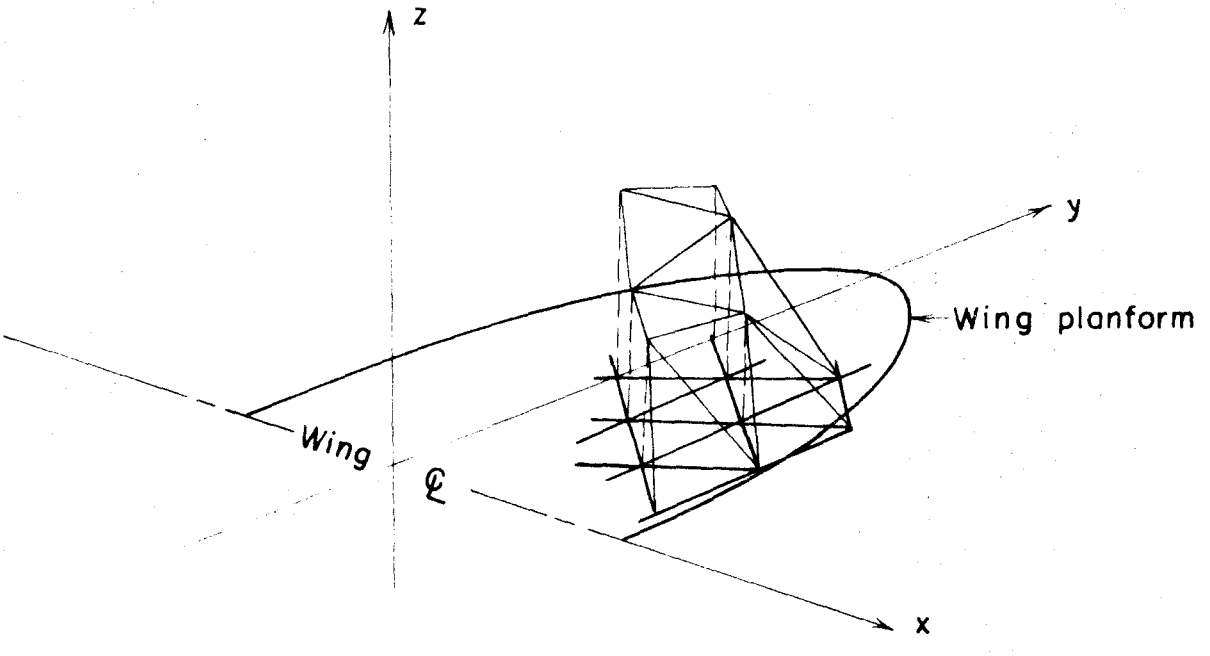

FIG. 24 - LINEAR-PRESSURE TRIANGLE CONSTRUCTION OF WING MODEL